Physics based basis function for vibration analysis of high speed rotating beams

R. Ganesh and Ranjan Ganguli*

Department of Aerospace Engineering, Indian Institute of Science, Bangalore 560012, India

Abstract.   The natural frequencies of continuous systems depend on the governing partial differential equation and can be numerically estimated using the finite element method. The accuracy and convergence of the finite element method depends on the choice of basis functions. A basis function will generally perform better if it is closely linked to the problem physics. The stiffness matrix is the same for either static or dynamic loading, hence the basis function can be chosen such that it satisfies the static part of the governing differential equation. However, in the case of a rotating beam, an exact closed form solution for the static part of the governing differential equation is not known. In this paper, we try to find an approximate solution for the static part of the governing differential equation for an uniform rotating beam. The error resulting from the approximation is minimized to generate relations between the constants assumed in the solution. This new function is used as a basis function which gives rise to shape functions which depend on position of the element in the beam, material, geometric properties and rotational speed of the beam. The results of finite element analysis with the new basis functions are verified with published literature for uniform and tapered rotating beams under different boundary conditions. Numerical results clearly show the advantage of the current approach at high rotation speeds with a reduction of 10 to 33% in the degrees of freedom required for convergence of the first five modes to four decimal places for an uniform rotating cantilever beam.

Keywords: rotating beam; finite element method; basis functions; shape function; turbine blade

1. Introduction

   The dynamics of rotating beams is an important area of research as many practical engineering structures such as helicopter rotor blades, gas turbine blades etc. can be modeled as rotating beams (Pnueli 1972, Fox and Burdess 1979, Hodges and Rutkowski 1981, Wright *et al*. 1982, Bauchau and Hong 1987, Fallahi *et al*. 1994, Bazoune and Khulief 1992, Hamdan and Al-Bedoor 2001). The variation of centrifugal force along the length of the beam causes a stiffening effect leading to a variation in the response of the beam from what it would have been for a non-rotating condition. The natural frequency of the beam is a very important factor in design considerations for practical applications as external forcing at the natural frequencies might cause resonance in the system which is not desired. Theoretically, any beam has infinite modes of vibration but it has been observed that only the first few modes contribute significantly to the response of the system

*Corresponding author, Professor, E-mail: ganguli@aero.iisc.ernet.in

(Subrahmanyam and Kaza 1987, Udupa and Varadan 1990, Naguleswaran 1994, Lee and Kuo 1992, Yokoyama 1988, Lin 2001, Pesheck *et al*. 2002, Lin and Lee 2004, Kim 2006, Bazoune *et al*. 1999). In the case of rotating beams, the first 2-5 modes are considered for vibration analysis. In these modes, it is observed that the centrifugal stiffness dominates the first two modes and in the higher modes the flexural stiffness dominates the response of the system.

A general physical system can be described in terms of partial differential equations. For many practical systems, the partial differential equations are linear and the natural frequencies are obtained by the method of separation of variables by assuming a solution of the form $w(x, t) = W(x)e^{i\omega t}$ where ω is the natural frequency. For some simple systems such as an uniform non-rotating beam, the resulting ordinary differential equation can be solved exactly for the natural frequency using appropriate boundary conditions. However, for many physical systems such as the rotating beam, an exact solution is not possible and approximate methods such as the Rayleigh Ritz, Galerkin and finite element method need to be used. Another approach is to use a Frobenius series solution of the differential equation and the dynamic stiffness method (Hashemi *et al*. 1999, Banerjee 2000, Huang and Liu, 2001, Gupta and Manohar, 2002, Wang and Wereley 2004). However, the finite element method is most popular in engineering due to its ease of computer implementation and adaptability to non-uniform cross sections. The finite element method converts the ordinary differential equations into matrix equations through a spatial discretization of the physical domain. The natural frequencies of any physical system are then obtained by the solution to the generalized eigenvalue problem $\mathbf{K}\phi = \lambda \mathbf{M}\phi$. The matrices $\mathbf{K}$ and $\mathbf{M}$ are formed using the finite element method.

In the finite element method, we assume the displacement variation in the element to be interpolated in terms of the values of displacement and slopes at nodal points specified within the element. The interpolation functions can be obtained by assuming a basis function for the displacement variation in the element. The basis function is generally assumed to be a polynomial and these basis functions show asymptotical convergence i.e., either making the discretization finer or assuming a higher polynomial approximation (increasing the number of nodes) improves the accuracy of the method.

The convergence of finite element methods can be improved if we assume basis functions which will closely resemble the displacement variation in the physical problem (Chakraborty *et al*. 2003, Cook *et al*. 2002, Reddy 1993). The stiffness matrix for dynamic analysis of any structural system is same as that in static analysis. Hence a very good choice for basis functions is one which satisfies the static part of the governing partial differential equation. In the case of rotating beams, an analytical solution for the static part of the governing partial differential equation is not known. In order to simplify the analysis, the cubic polynomial which is the solution to the static part of differential equation of a non-rotating beam is generally chosen as the basis function. Since the flexural stiffness dominates the response of the system in the higher modes, the cubic polynomial captures the higher modes very effectively. However, they do not capture the first few modes effectively and show slow convergence for the first few modes especially at higher rotation speeds.

Several researchers (Gunda *et al*. 2007, Gunda and Ganguli 2008a, b, Al-Qaisia and Al-Bedoor 2005) have tried to simplify the governing equation such that an exact analytical solution can be found for the equation. It has been observed that these modified basis functions show improved convergence for the fundamental mode but converge slower than the cubic functions for the higher modes. The present paper addresses this problem by developing new physics based basis functions for rotating beams.

In order to obtain improved convergence for all the modes, the basis function must be able to

capture the effects of the flexural stiffening as well as include the centrifugal stiffening effect. The centrifugal force varies along the length of the beam (maximum at the root and zero at the tip), hence the stiffness of the system varies along the length of the beam too. We try to split the static part of the differential equation into the flexural and the centrifugal part. This indirectly represents the analysis of a non-rotating beam and a rotating string separately. We assume a solution to the differential equation to be a linear combination of the two separate solutions. A method for solving differential equations is the collocation method (Wright 2007). In this method, we assume an approximate solution which is either defined in the global domain or in a piecewise manner and then use the residual in the differential equation to solve for the constants in the solution. We define an approximation in a given number of subintervals and then obtain a relation for the solution usingthe collocation method. This approximated solution is then used as a basis function in the finite element method.

Conventional finite element methods do not directly take the error into account. Gunda and Ganguli (2008b) tried to use the local form of differential equation for obtaining the shape functions and showed that improved convergence was not obtained in the higher modes. The combination of the collocation and the finite element method is what gives the current method the advantage over conventional finite element methods.

2. Basis function

The schematic of a rotating tapered beam is shown in Fig. 1. The governing differential equation of a Euler-Bernoulli rotating beam is given by Hodges and Rutkowski (1981).

$$\frac{\partial^2}{\partial x^2}\left(EI(x)\frac{\partial^2 w}{\partial x^2}\right) - \frac{\partial}{\partial x}\left(T(x)\frac{\partial w}{\partial x}\right) + m(x)\frac{\partial^2 w}{\partial t^2} = 0 \tag{1}$$

where $EI(x)$ is the flexural stiffness, $T(x)$ is the axial force due to centrifugal stiffening, $m(x)$ is the mass per unit length of the beam, w is the bending displacement and is the rotation speed.

The axial force due to centrifugal stiffening, $T(x)$ is given as

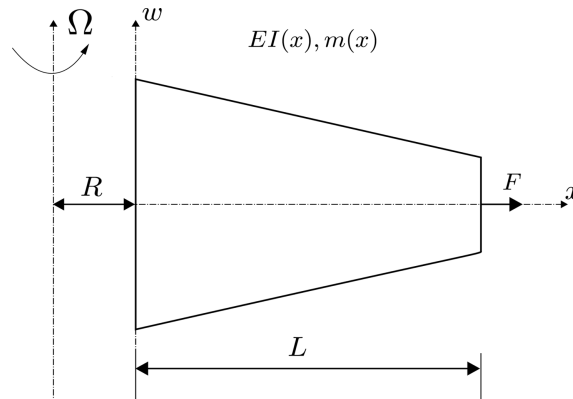$$T(x) = \int_x^L m(x)\Omega^2(R+x)dx + F \tag{2}$$

Fig. 1 Rotating beam

where R is the hub radius, L is the length of the beam and F is the axial force acting at the end of the beam. The static homogenous part of the governing differential equation for a rotating beam is obtained by ignoring the inertia term in Eq. (1) and is given by

$$\frac{d^2}{dx^2}\left(EI(x)\frac{d^2w}{dx^2}\right) - \frac{d}{dx}\left(T(x)\frac{dw}{dx}\right) = 0 \tag{3}$$

Eq. (3) does not have an exact closed form solution. Series solution for Eq. (3) can be considered but Wang and Wereley (2004) have shown that as many as 350 terms in the series solution have to be included for the Frobenius solution to give superior convergence for the rotating beam problem. In order to find an approximate solution, we assume $EI(x)$ and $m(x)$ to be constant. Furthermore, using $R = F = 0$, Eq. (3) can be simplified to

$$EI\frac{d^4w}{dx^4} - \frac{m\Omega^2}{2}\frac{d}{dx}\left((L^2 - x^2)\frac{dw}{dx}\right) = 0 \tag{4}$$

The equation can be further simplified by introducing a dimensionless parameter $\lambda^2 = m\Omega^2 L^4/EI$

$$\frac{d^4w}{dx^4} - \frac{\lambda^2}{2L^4}\frac{d}{dx}\left((L^2 - x^2)\frac{dw}{dx}\right) = 0 \tag{5}$$

We try to find an approximate solution to the static part of the governing differential equation by splitting Eq. (5) into two parts; the centrifugal part and the flexural part. For the equation to have an exact solution, we assume that a function w exists such that both the parts are satisfied i.e., both the operators must go to zero.

$$\frac{d^4w}{dx^4} = 0 \tag{6}$$

$$\frac{d}{dx}\left((L^2 - x^2)\frac{dw}{dx}\right) = 0 \tag{7}$$

The cubic function satisfies Eq. (6)

$$\frac{d^4w}{dx^4} = 0 \Rightarrow w^{(1)} = a_0 + a_1 x + a_2 x^2 + a_3 x^3 \tag{8}$$

Eq. (8) represents the case of a non-rotating beam.
If we try to satisfy the centrifugal part given by Eq. (7) we get

$$\frac{d}{dx}\left((L^2 - x^2)\frac{dw}{dx}\right) = 0 \Rightarrow w^{(2)} = a\ln\left(\frac{L+x}{L-x}\right) \tag{9}$$

Eq. (9) represents the case of a rotating string with no stiffness (Hildebrand 1965). As the rotation speed of the beam increases, the centrifugal effects overwhelm the flexural stiffness and the rotating beam approaches the rotating string. It is reasonable to assume that a rotating beam solution should satisfy the extreme cases where rotation speed is zero and rotation speed is very high. Therefore, we consider a linear combination of Eq. (8) and Eq. (9) as a solution to Eq. (3)

$$W_a = a_0 + a_1 x + a_2 x^2 + a_3 x^3 + a_4\ln\left(\frac{L+x}{L-x}\right) \tag{10}$$

Any fourth order differential equation can have only four constants which can be found using the boundary conditions. Eq. (10) contains an extra constant a_4; hence we eliminate a_4 from the solution by using an idea from the collocation method. The collocation method is an approach for solving differential equations by assuming a solution and finding the values of constants in the solution by forcing the differential equation to be satisfied at several 'collocation' points in the domain. The residual arising in the differential equation by assuming Eq. (10) to be a solution to Eq. (3) is given by

$$\varepsilon = EI\frac{d^4W_a}{dx^4} - \frac{m\Omega^2}{2}\frac{d}{dx}\Big((R(L-x)+(L^2-x^2))\frac{dW_a}{dx}\Big) \tag{11}$$

We set the error to zero at some points z within the domain

$$\varepsilon(z) = 0 \Rightarrow W_a = a_0 + a_1 x + a_2 x^2 + a_3 x^3 + f(a_0, a_1, a_2, a_3, z)\ln\Big(\frac{L+x}{L-x}\Big) \tag{12}$$

where z represents points within the domain $(0, L)$. We have considered the open interval because the natural and essential boundary conditions are imposed at the ends of the beam.

Until now, we have discussed on obtaining and approximate solution to the static part of the governing differential equation for a rotating beam. In order to use this solution as a basis function for the finite element method, the static part of the governing differential equation for the ith element shown in Fig. 1 is given by

$$\frac{d^2}{d\bar{x}^2}\Big(EI(x_i+\bar{x})\frac{d^2 w_i}{d\bar{x}^2}\Big) - \frac{d}{d\bar{x}}\Big(T(x_i+\bar{x})\frac{dw_i}{d\bar{x}}\Big) = 0 \tag{13}$$

Using similar techniques as explained for Eq. (3)

$$w = a_0 + a_1(x_i+\bar{x}) + a_2(x_i+\bar{x})^2 + a_3(x_i+\bar{x})^3 + a_4\ln\Big(\frac{L+x_i+\bar{x}}{L-x_i-\bar{x}}\Big) \tag{14}$$

Eq. (14) can be further simplified as

$$w = c_0 + c_1\bar{x} + c_2\bar{x}^2 + c_3\bar{x}^3 + c_4\ln\Big(\frac{L+x_i+\bar{x}}{L-x_i-\bar{x}}\Big) \tag{15}$$

We recall that the mass and flexural variation was assumed to be a constant in obtaining the solution given by Eq. (15). This assumption is validated by the fact that in the limit of mesh refinement the mass and flexural variation can be neglected. Hence, even though the solution was obtained for an uniform beam, it is used only for the finite element and is valid for all classes of tapered beams.

When we choose Eq. (11) as a basis function, it requires substitution at $x = l$ which will give rise to a discontinuity at the last element. Now, in order to simplify the finite element calculations, we approximate the equation as

$$w = c_0 + c_1\bar{x} + c_2\bar{x}^2 + c_3\bar{x}^3 + c_4\ln\Big(\frac{L+\bar{x}}{L-\bar{x}}\Big) \tag{16}$$

We can presume that the above approximation to the basis function will be negated by choosing a finer discretization of our beam, which is typical of finite element methods. Consider a two-noded four degree of freedom element shown in Fig. 2. For the sake of brevity, we give the solution for
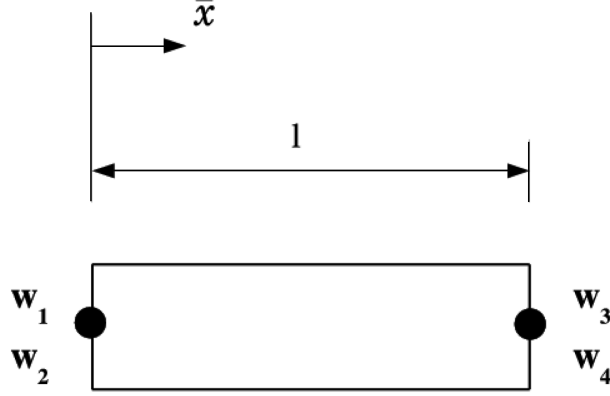
Fig. 2 Finite element model

$R = 0$. The boundary conditions for the element are given by

$$w = c_0 + c_1\bar{x} + c_2\bar{x}^2 + c_3\bar{x}^3 + c_4\ln\left(\frac{L+\bar{x}}{L-\bar{x}}\right) \tag{17}$$

$$w(0) = c_0 = w_1 \tag{18}$$

$$\frac{dw(0)}{d\bar{x}} = \frac{2c_4}{L} = w_2 \tag{19}$$

$$w(l) = c_0 + c_1 l + c_2 l^2 + c_3 l^3 + c_4\ln\left(\frac{L+l}{L-l}\right) = w_3 \tag{20}$$

$$\frac{dw(l)}{d\bar{x}} = c_1 + 2c_2 l + 3c_3 L^2 + \frac{2c_4 L}{(L^2-l^2)} = w_4 \tag{21}$$

where

$$c_4 = \frac{(L^2-z^2)^4 \lambda^2 (L^2 c_2 + (3c_3 L^2 - c_1)z - 3c_2 z^2 - 6c_3 z^3)}{48L^5 z (L^2-z^2)} \tag{22}$$

Eq. (22) is obtained by solving Eq. (12).

Since the basis function defined by Eq. (17) contains polynomial terms upto order three, it can represent a rigid body mode as well as a state of constant strain. Hence the above basis function will give rise to a complete interpolation polynomial (Bathe 1996).

We set the error to zero at a collocation point within the element. We choose $\bar{x} = l/2$ within each element so that for any general element this point will be $z = x_i + l/2$. Since we assume an uniform mesh $x_i = (i-1)l$, the zero error condition holds within each element(i) at

$$z = (i-1/2)l \tag{23}$$

From Eqs. (17)-(23), the constants c_0, c_1, c_2, c_3 can be solved and the displacement function can be written in terms of the displacements and slopes at the nodes.

$$w = N_1 w_1 + N_2 w_2 + N_3 w_3 + N_4 w_4 \tag{24}$$

where N_1, N_2, N_3, N_4 are the interpolating functions and are given as

$$N_1 = \frac{R_1}{D}, \quad N_2 = \frac{R_2}{D}, \quad N_3 = \frac{R_3}{D}, \quad N_4 = \frac{R_4}{D}$$

where

$$R_1 = l(12L\lambda^2(L^2-z^2)^4(L^2-l^2)(2L^2z-L^2l-4z^3+3lz^2)\left(\ln\left(\frac{L+\overline{x}}{L-\overline{x}}\right)-\ln\left(\frac{L+l}{L-l}\right)-(l-\overline{x})\right.$$

$$(12\lambda^2(2L^2-l(l-\overline{x}))z^{11}+l\lambda^2z^8(3L^2-(2l+\overline{x})((l-\overline{x}))(26L^2-6z^2)-2\lambda^2z^9(54L^4-2L^2$$

$$(14l+\overline{x})(l-\overline{x})+(l+\overline{x})(l-\overline{x})l^2)+8L^2\lambda^2z^7(24L^4-(l-\overline{x})(13l+\overline{x})L^2+(l+\overline{x})(l-\overline{x})l^2)-44L^4l$$

$$(3L^2-(2l+\overline{x})(l-\overline{x})))\lambda^2z^6-12L^4\lambda^2z^5(l^2(l+\overline{x})(l-\overline{x})+14L^4-(4l+\overline{x})(l-\overline{x})L^2)-36L^6l$$

$$\lambda^2z^4((2l+\overline{x})(l-\overline{x})-3L^2)+4L^6z^3(18\lambda^2L^4-((11l+4\overline{x})\lambda^2+24\overline{x}+12l)(1-\overline{x})L^2+2(6+\lambda^2)l^2$$

$$(1+\overline{x})(1-\overline{x}))+14L^8l\lambda^2z^2((2l+\overline{x})(1-\overline{x}))-3L^2)-2L^8z(6\lambda^2L^4-2(1-\overline{x})((2l+\overline{x})\lambda^2-24\overline{x}$$

$$-12l)L^2+l^2(l+\overline{x})(l-\overline{x})(-24+\lambda^2))+2L^{10}l\lambda^2(3L^2-(\overline{x}+2l)(l-\overline{x}))) \tag{25}$$

$$R_2 = L((L^2-z^2)^4\lambda^2(L^2-l^2)\overline{x}(12l-6\overline{x})z^3-(9l^2-3\overline{x}^2)z^2-((6l-3\overline{x})L^2+2l\overline{x}^2-3\overline{x}l^2)z+L^2(3l^2$$

$$-\overline{x}^2))\ln\left(\frac{L+l}{L-1}\right)-l\left((L^2-z^2)^4\left(6z^3-6lz^2+(-3L^2+l^2)z+L^2l\right)l\lambda^2(L^2-l^2)\ln\left(\frac{L+\overline{x}}{L-\overline{x}}\right)\right.$$

$$-(6\lambda^2z^{11}-3\lambda^2(l+\overline{x})z^{10}-\lambda^2(27L^2-\overline{x}l)z^9+13L^2\lambda^2(l+\overline{x})z^8+4L^2\lambda^2(12L^2-\overline{x}l)z^7+22\lambda^2L^4$$

$$(l+\overline{x})z^6+6\lambda^2L^4(7L^2-\overline{x}l)z^5-18L^6\lambda^2(l+\overline{x})z^4-2L^6z(9\lambda^2L^4-2l(6l-6\overline{x}+\overline{x}\lambda^2)L^2$$

$$+12l^3(l-\overline{x}))L^4z^3+7L^8\lambda^2(l+\overline{x})z^2+(3\lambda^2L^4-l(24l-\overline{x}\lambda^2-24\overline{x})L^2+24l^3(l-\overline{x}))-L^{10}\lambda^2$$

$$(l+\overline{x}))2L\overline{x}(l-\overline{x}))) \tag{26}$$

$$R_3 = l\left(L\lambda^2(L^2-l^2)(L^2-z^2)^4\ln\left(\frac{L+\overline{x}}{L-\overline{x}}\right)(12z^3-9lz^2+3L^2l-6L^2z)-2\overline{x}(-6\lambda^2(2L^2-(2l-\overline{x})l)\right.$$

$$z^{11}+3\lambda^2lz^{10}(3L^2-3l^2+\overline{x}^2)+\lambda^2(54L^4+(2\overline{x}^2-54l^2+24l\overline{x})L^2+\overline{x}l^2(3l-2\overline{x}))z^9+L^2\lambda^2$$

$$lz^6(3L^2-l^2+\overline{x}^2)(11L^2-13z^2)+\overline{x}l^2(3l-2\overline{x})+4L^2\lambda^2(24L^4+(2\overline{x}^2+9l\overline{x}-24l^2)L^2)z^7$$

$$+6L^4\lambda^2z^5(14L^4+(4l\overline{x}+2\overline{x}^2-14l^2)L^2+\overline{x}l^2(3l-2\overline{x}))+18L^6\lambda^2lz^4(\overline{x}^2-3l^2+3L^2)$$

$$+2L^6z^3(18\lambda^2L^4+((4\overline{x}^2-18l^2+3l\overline{x})\lambda^2+24\overline{x}^2-36l\overline{x})L^2+2\overline{x}l^2(6+\lambda^2)(3l-2\overline{x}))$$

$$+7l^8(\overline{x}^2-3l^2+3L^2)\lambda^2lz^2-L^8z(6\lambda^2L^4+((2\overline{x}^2-6l^2)\lambda^2-48\overline{x}^2+72l\overline{x})L^2+\overline{x}l^2(\lambda^2-24)$$

$$(3l-2\overline{x}))-\lambda^2L^{10}l(\overline{x}^2-3l^2+3L^2)) \tag{27}$$

$$R_4 = (L^2 - l^2)\Big(L\lambda^2\bar{x}^2((-3z+\bar{x})L^2 + (2z-\bar{x})3z^2)(L^2-z^2)^4\ln\Big(\frac{L+l}{L-l}\Big) + l(L\lambda^2 l((3z-l)L^2 - 3z^2$$

$$(2z-l))(L^2-z^2)^4\ln\Big(\frac{L+\bar{x}}{L-\bar{x}}\Big) - 2(\lambda^2 L^{10}(3z-l-\bar{x}) - zL^8(\lambda^2(18z^2 - 7(l+\bar{x})z - l\bar{x}) - 24l\bar{x})$$

$$+ 2((21z^2 - 9(l+\bar{x})z + 2l\bar{x})\lambda^2 + 12l\bar{x})z^3 L^6 - 2\lambda^2 z^5 L^4(24z^2 - 11(l+\bar{x})z + 3l\bar{x}) + \lambda^2 z^7 L^2(27z^2$$

$$+ 4l\bar{x} - 13(l+\bar{x})z) - \lambda^2(6z^2 - 3(l+\bar{x})z + l\bar{x})z^9)\bar{x}(l-\bar{x}))) \qquad (28)$$

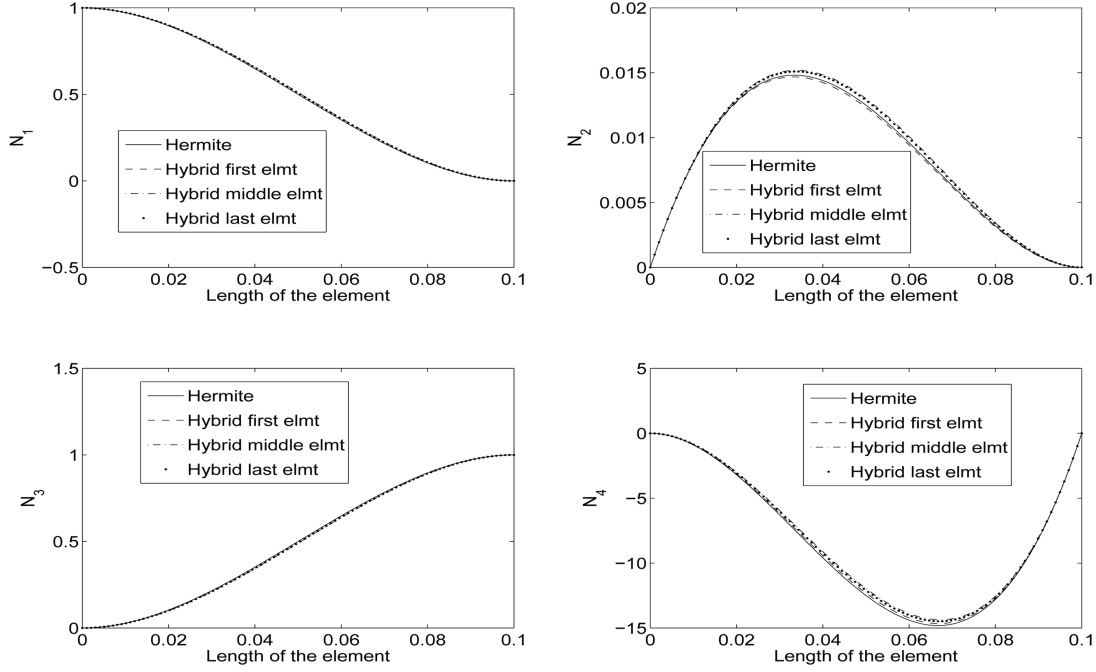$$D = l\Big((L^2-z^2)^4\lambda^2 L((l-2z)L^2 + (4z-3l)z^2)(L^2-l^2)\ln\Big(\frac{L+l}{L-l}\Big) - 2(3\lambda^2(l-2z)L^{12} + L^{10}$$

$$((4l^2z - 21lz^2 - 2l^3 + 36z^3)\lambda^2 - 24l^2z) - zL^8(\lambda^2(l^4 + 84z^4 + 22l^2z^2 - 14l^3z - 54lz^3)$$

$$- 24l^4 + 24l^2z^2) + 2z^3 L^6(\lambda^2(l^4 + 24z^4 + 12l^2z^2 - 33lz^3 - 18l^3z) + 6l^4) - \lambda^2 z^5 L^4(-44l^3z$$

$$+ 54z^4 + 6l^4 + 52l^2z^2 - 39lz^3) - \lambda^2(-9lz^3 + 12z^4 + 4l^4 - 26l^3z + 28l^2z^2)z^7 L^2 - l^2\lambda^2 z^9$$

$$(l^2 - 6zl + 6z^2))l) \qquad (29)$$

In the above equations $z = (i - 1/2)l$, $i = 1 \dots n_e$ represents the position of the element in the beam and $L = ln_e$.

The interpolating functions obtained here are a function of the material properties (EI, m), geometric properties (L) and rotational speed (Ω) of the beam. They also depend on the position of the element in the beam (x_i). Though the new basis functions appear quite complicated, the behavior of the shape functions is smooth and continuous in the beam which can be observed by plotting them. Figs. 3 and 4 show comparison of the shape functions of the first, middle and the last element using the hybrid basis function with the Hermite cubic shape functions at low and high rotation speeds, respectively, for a 10 element discretization ($n_e = 10$). At $\lambda = 12$, the shape functions are almost identical to the Hermite cubics showing that the effect of rotation is very small at low rotation speeds. The shape functions show increasing difference at the higher speed ($\lambda = 100$) and particularly near the root of the beam where the centrifugal effect is more (Eq. (2)). However, the effect of rotation is felt in the slope related shape functions N_2 and N_4 only and the displacement related functions show little change. The interpolating functions approach the Hermite cubic functions as the rotation speed tends to zero. The shape functions for the last element are almost similar to the Hermite cubic shape functions because the centrifugal force approaches zero.

It is verified mathematically that

$$\lim_{\lambda \to 0} N_1 = \frac{l^3 - 3\bar{x}^2 l + 2\bar{x}^3}{l^3}$$

$$\lim_{\lambda \to 0} N_2 = \frac{\bar{x}l^2 - 2\bar{x}^2 l + \bar{x}^3}{l^2}$$

$$\lim_{\lambda \to 0} N_3 = \frac{3\bar{x}^2 l - 2\bar{x}^3}{l^3}$$

$$\lim_{\lambda \to 0} N_4 = \frac{-\bar{x}^2 l + \bar{x}^3}{l^2}$$

Fig. 3 Comparison of shape function values for $\lambda = 12$ for different elements in the beam

3. Finite element analysis

The mass and stiffness matrices can be obtained using the energy expressions. The kinetic energy for a rotating beam is given by Reddy (1993)

$$T = \frac{1}{2} \int_0^L m(x) [\dot{w}(x,t)]^2 dx \tag{30}$$

where $\dot{w}(x,t)$ is the derivative of $w(x,t)$ with respect to time t.

The potential/strain energy is given by

$$U = \frac{1}{2} \int_0^L EI(x) [w''(x,t)]^2 dx + \frac{1}{2} \int_0^L T(x) [w'(x,t)]^2 dx \tag{31}$$

where $T(x)$ is defined in Eq. (2).

The mass and stiffness matrices (M_i and K_i) for a beam element can be obtained from the above energy expressions. The calculations for these matrices involve calculating the value of the following integrals.

$$M_i = \int_0^l m_i(\overline{x}) N^T N d\overline{x} \tag{32}$$

$$K_i = \int_0^l EI_i(\overline{x}) (N'')^T N'' d\overline{x} + \int_0^l T_i(\overline{x}) (N')^T N' d\overline{x} \tag{33}$$
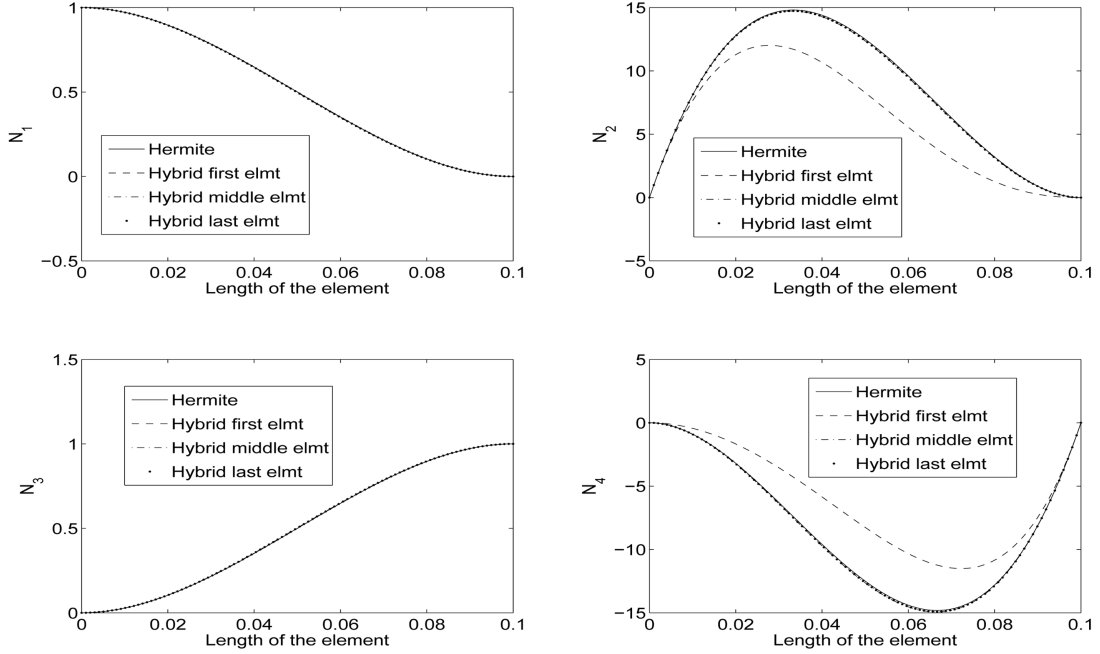
Fig. 4 Comparison of shape function values for $\lambda = 100$ for different elements in the beam

where

$$T_i(\bar{x}) = \int_{x_i + \bar{x}}^{l} m_i(\bar{x}) \Omega^2(\bar{x}) d\bar{x} \qquad (34)$$

No approximation is made in the variation of $EI(x)$ or $T(x)$ while calculating the mass and stiffness matrices. The assumptions have been made only to derive the new basis functions. The mass and stiffness matrices are calculated for each element and then assembled into the global mass and stiffness matrix. These matrices are then used to determine the natural frequencies and the mode shapes by solving the eigenvalue problem.

$$\mathbf{K}\phi = \omega^2 \mathbf{M}\phi \qquad (35)$$

4. Numerical results

The new hybrid basis function is used in the free vibration analysis of rotating uniform and tapered beams with different boundary conditions and the results obtained are compared with published literature.

4.1 Uniform beam

In uniform rotating beams, $m(x)$ and $EI(x)$ are constant. Tables 1 and 2 show comparison of non-dimensional rotating frequencies of an uniform rotating cantilever and hinged beam with published

Table 1 Comparison of non-dimensional frequencies for cantilevered uniform rotating beam

Mode	Present FEM	Wang and Wereley (2004)	Wright *et al.* (1982)	Hodges and Rutkowski (1981)
1	13.1702	13.1702	13.1702	13.1702
2	37.6031	37.6031	37.6031	37.6031
3	79.6145	79.6145	79.6145	79.6145
4	140.534	140.534	140.534	N/A
5	220.536	220.536	220.536	N/A

Table 2 Comparison of non-dimensional frequencies for hinged uniform rotating beam

Mode	Present FEM	Wang and Wereley (2004)	Wright *et al.* (1982)
1	12.0002	12.0000	12.0000
2	33.7603	33.7603	33.7603
3	70.8373	70.8373	70.8373
4	126.431	126.431	126.431
5	201.123	201.122	201.122

Table 3 Comparison of number of elements and degrees of freedom required for convergence of natural frequencies with accuracy of 1e-4 for Cantilevered Uniform Rotating Beam

Modes	$\lambda = 12$		$\lambda = 100$	
	Hybrid function	Cubic function	Hybrid function	Cubic function
1	9(18)	12(24)	33(66)	58(116)
2	15(30)	16(32)	48(96)	69(138)
3	24(48)	24(48)	54(108)	77(154)
4	35(70)	35(70)	60(120)	84(168)
5	47(94)	47(94)	61(122)	91(182)

literature (Hodges and Rutkowski 1981, Wang and Wereley 2004, Wright *et al.* 1982). Hodges and Rutkowski (1981) used a variable order basis function in the finite element method while Wang and Wereley (2004) and Wright *et al.* (1982) used the Frobenius solution in the dynamic stiffness method to generate the natural frequencies of the rotating beam. We can see from Tables 1 and 2 that the current formulation gives identical results to the published literature.

Table 3 shows the comparison of the number of elements required for convergence of the first five modes upto four decimal places. The degrees of freedom is also specified in parentheses. The convergence of the formulation is compared with that of the Hermite cubic shape functions for two rotation speeds $\lambda = 12$ and $\lambda = 100$. It is seen that in the case of the cantilever beam, the hybrid function requires 47 elements for $\lambda = 12$ and 61 elements for $\lambda = 100$ to obtain converged values for the first five modes. For $\lambda = 12$, the Hermite cubic functions also require only 47 elements but for $\lambda = 100$ it requires 91 of elements for converged values of the first five modes. We can see that the hybrid basis functions give some advantage in the fundamental mode convergence at $\lambda = 12$, however, this advantage becomes clear at $\lambda = 100$ for all the five modes. Figs. 5 and 6 show the
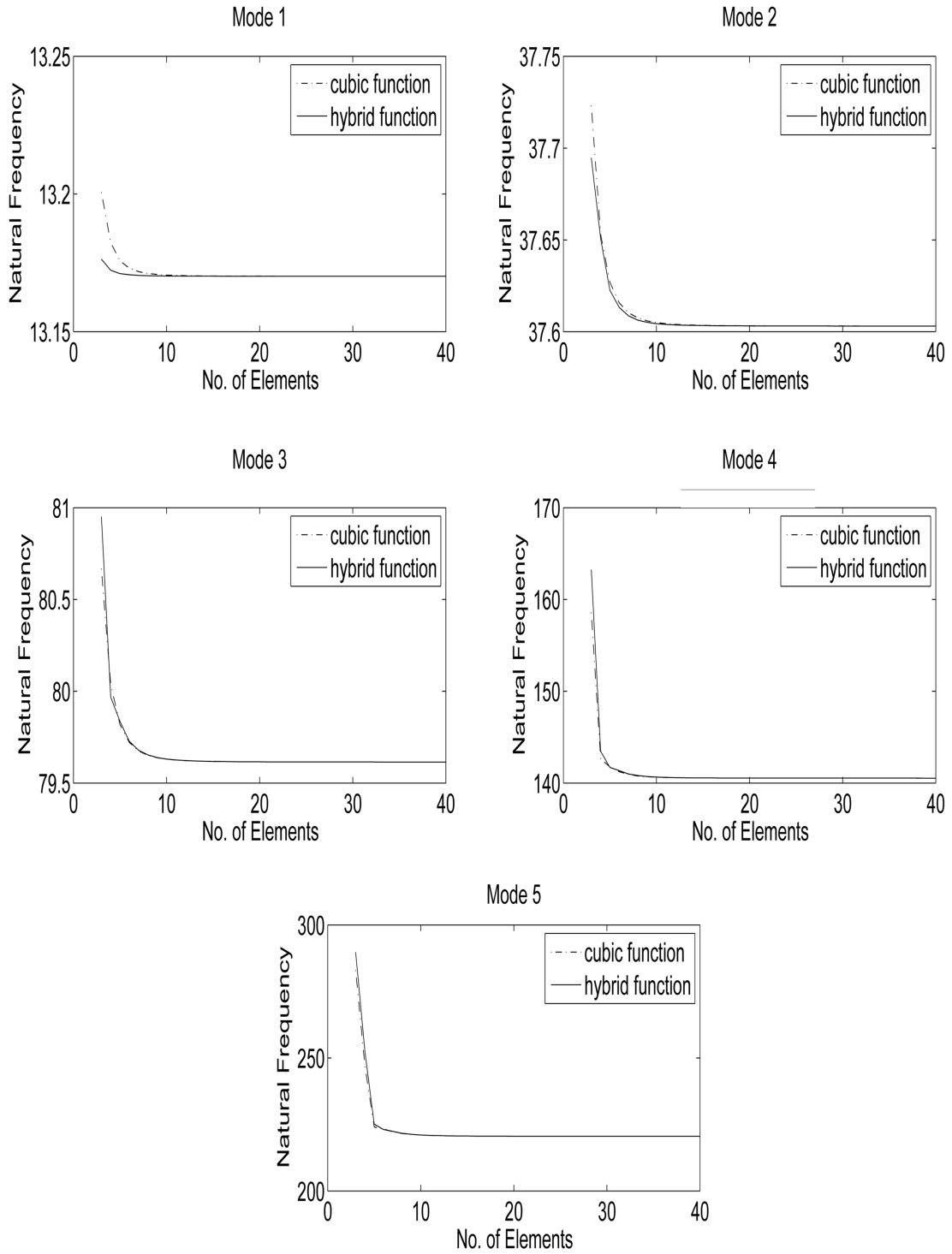
Mode 1

Mode 2

Mode 3

Mode 4

Mode 5

Fig. 5 Comparison of convergence of hybrid function and hermite cubic function for uniform cantilever beam with $\lambda = 12$
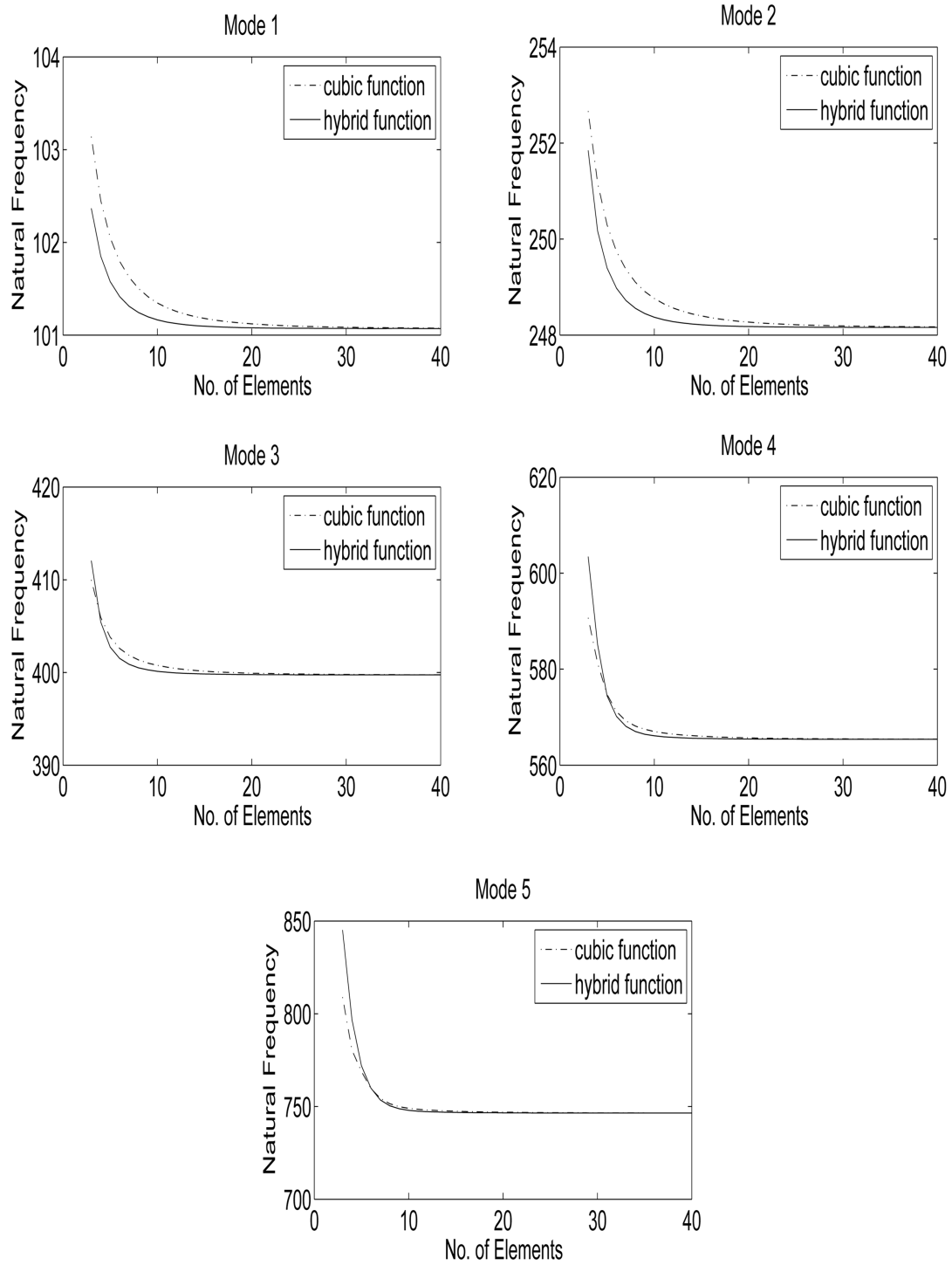
Fig. 6 Comparison of convergence of hybrid function and hermite cubic function for uniform cantilever beam with $\lambda = 100$

convergence of the natural frequencies with the hybrid and the cubic basis functions, at $\lambda = 12$ and $\lambda = 100$, respectively. In fact, with the new basis functions, a reduction of about 33% is obtained at $\lambda = 100$ in the number of elements required for convergence when compared to the cubic basis functions. The number of degrees of freedom is reduced from 182 to 122 at $\lambda = 100$, which considerably reduces the eigenvalue problem size and makes the new basis functions attractive for the vibration analysis of high speed rotating beams.

The accuracy of the current hybrid function is observed by considering the difference in the value of natural frequency obtained for a very coarse discretization of the beam with the converged value of the natural frequency. This difference is a measure of the error. Table 4 shows a comparison of the difference in values of the non-dimensional natural frequency obtained by using the hybrid and

Table 4 Comparison of difference in the value of non-dimensional natural frequency obtained by using the Hybrid and the Cubic function for a low discretization in the FEM with the converged value for $\lambda = 100$

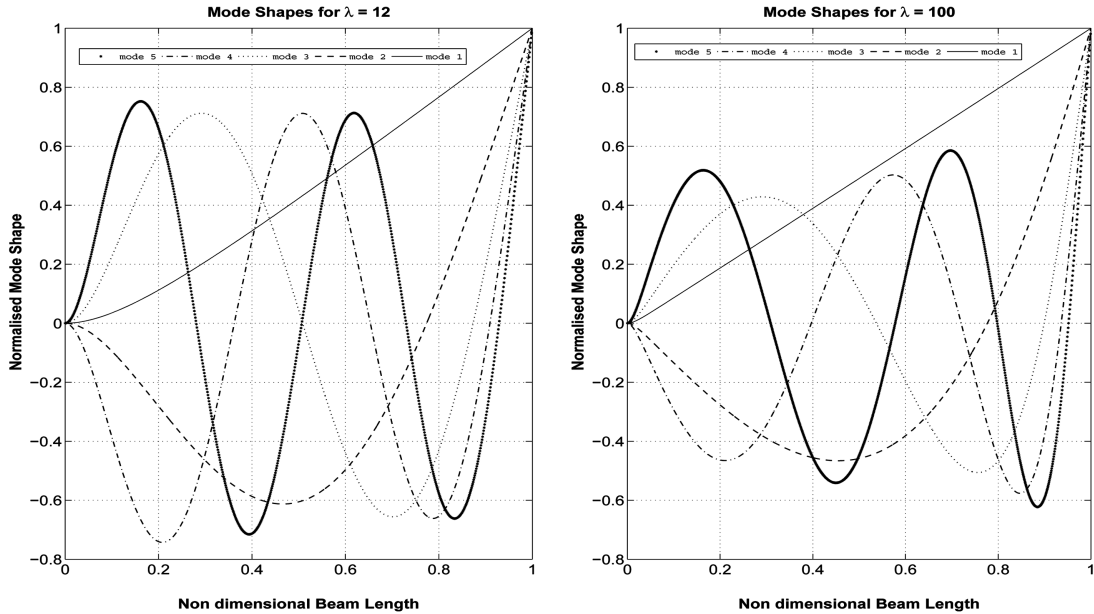| Mode	$n_e = 3$		$n_e = 7$		$n_e = 10$		$n_e = 20$	
	Hybrid function	Cubic function	Hybrid function	Cubic function	Hybrid function	Cubic function	Hybrid function	Cubic function
1	1.2961	2.0705	0.2417	0.5537	0.0941	0.2674	0.0088	0.0506
2	3.6876	4.5076	0.5615	1.2076	0.2125	0.6036	0.0193	0.1107
3	12.3151	10.2412	1.1423	2.1143	0.3928	1.0291	0.0355	0.1898
4	38.0513	25.3037	2.6878	3.8457	0.7370	1.6412	0.0669	0.3018
5	98.7069	62.4297	7.1107	7.9247	1.4760	2.5897	0.1298	0.4559

Fig. 7 Eigen mode shapes with the hybrid basis function for uniform cantilever beam with (a) $\lambda = 12$, (b) $\lambda = 100$
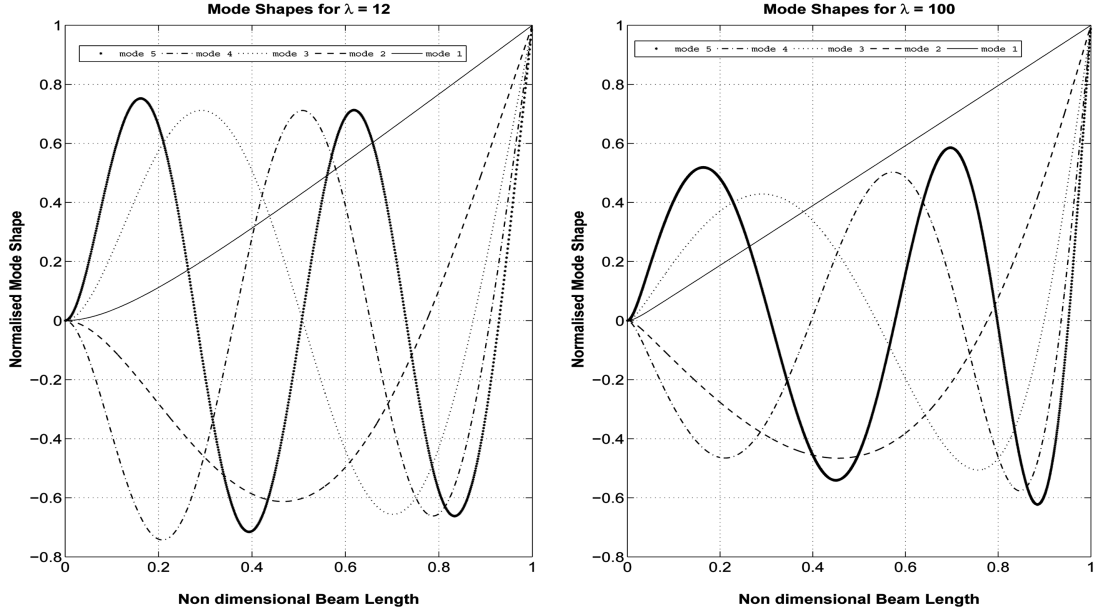
Fig. 8 Eigen mode shapes with the hermite cubic basis function for uniform cantilever beam with (a) $\lambda = 12$, (b) $\lambda = 100$

the cubic function for a coarse discretization. At least a three element discretization is necessary to obtain the natural frequency for the first five modes. With a three element discretization, it is observed that the difference in the value obtained and the converged value is less for the first two modes when we use the current hybrid function. When the beam is discretized into seven elements, the current basis function shows better accuracy for all the five modes when compared to the cubic basis function. Thus we can construct low order models of the rotating beam which are often useful in control applications, using the new basis functions. Wang and Wereley (2004) mention that the creation of low order models is critical for control of rotating beams when smart materials based actuation is used. For the 10 and 20 element cases, the new hybrid shape functions also perform better than the Hermite cubic's for all the five modes.

Fig. 7 shows the Eigen Mode shapes obtained with the current hybrid function for $\lambda = 12$ and $\lambda = 100$. The mode shapes obtained by using the Hermite cubic shape functions is shown in Fig. 8. It is seen that the hybrid function is able to capture the mode shapes accurately especially for the fundamental mode which becomes linear as the rotation speed becomes considerably high. In such situations, the centrifugal force dominates the whole response of the system thereby making it behave similar to rotating string.

4.2 Tapered beam

For a tapered beam, we assume that the variation of mass along the beam is given by

$$m = m_0(1 - \alpha \xi) \tag{36}$$

where m_0 corresponds to the value of mass per unit length at the thick end of the beam ($\xi = 0$), α is the taper parameter such that $0 < \alpha < 1$, ξ is the non-dimensional length of the beam : $\xi = x/L$.

The flexural stiffness variation along the tapered beam is given by

$$EI = EI_0(1 - \beta_1\xi - \beta_2\xi^2 - \beta_3\xi^3 - \beta_4\xi^4) \tag{37}$$

where EI_0 corresponds to the value of flexural rigidity at the thick end of the beam ($\xi = 0$), β_i, $i = 1 \dots 4$ are taper parameters for the stiffness distribution. These parameters can be determined by using for beams with a rectangular cross section and thickness varying along the length. However, it is not necessary that the taper and mass parameters be related and the only condition is that they should not give rise to a singularity at ($\xi = 1$). In order to validate the current formulation we consider two special cases of Eqs. (36) and (37) and verify the results with published literature.

4.2.1 Linear mass and linear stiffness beam

We assume $m(x) = m_0(1 - 0.8x)$ and $EI(x) = EI_0(1 - 0.95x)$. Tables 5 and 6 show comparison of non-dimensional rotating frequencies of a cantilever and hinged beam with published literature (Wang and Wereley 2004, Wright *et al.* 1982). The results compare very well with published literature.

Figs. 9 and 10 show the comparison of the convergence rate of the current shape functions with the Hermite Cubic Shape functions. For the low speed case ($\lambda = 12$) the current basis function do not show improvement over the cubic polynomial. But in the higher speed case ($\lambda = 100$), the new function shows improved convergence.

Table 5 Comparison of non-dimensional frequencies for linear mass, linear stiffness cantilevered rotating beam

Mode	Present FEM	Wang and Wereley (2004)	Wright *et al.* (1982)
1	14.0313	14.0313	14.0313
2	35.9064	35.9060	35.9064
3	72.8565	72.8565	72.8565
4	126.401	126.336	126.401
5	198.880	198.243	198.880

Table 6 Comparison of non-dimensional frequencies for linear mass, linear stiffness hinged rotating beam

Mode	Present FEM	Wang and Wereley (2004)	Wright *et al.* (1982)
1	12.0000	12.0000	12.0000
2	30.7745	30.7741	30.7745
3	63.1722	63.1758	63.1722
4	112.090	112.040	112.090
5	178.016	178.978	178.105

Mode 1
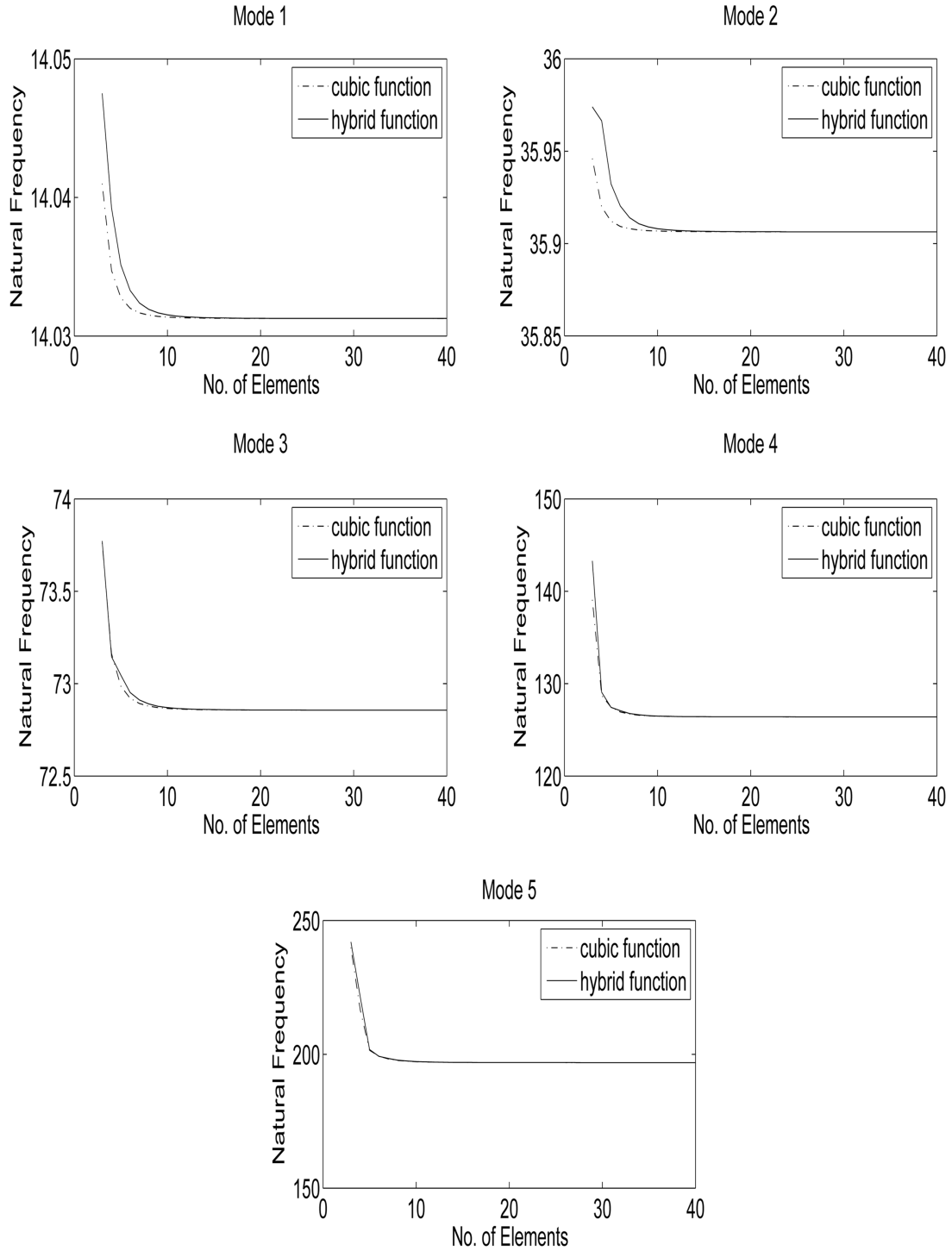
Mode 2

Mode 3

Mode 4

Mode 5

Fig. 9 Comparison of convergence of hybrid function and hermite cubic function for linearly tapered, linear flexural stiffness cantilever beam with $\lambda = 12$
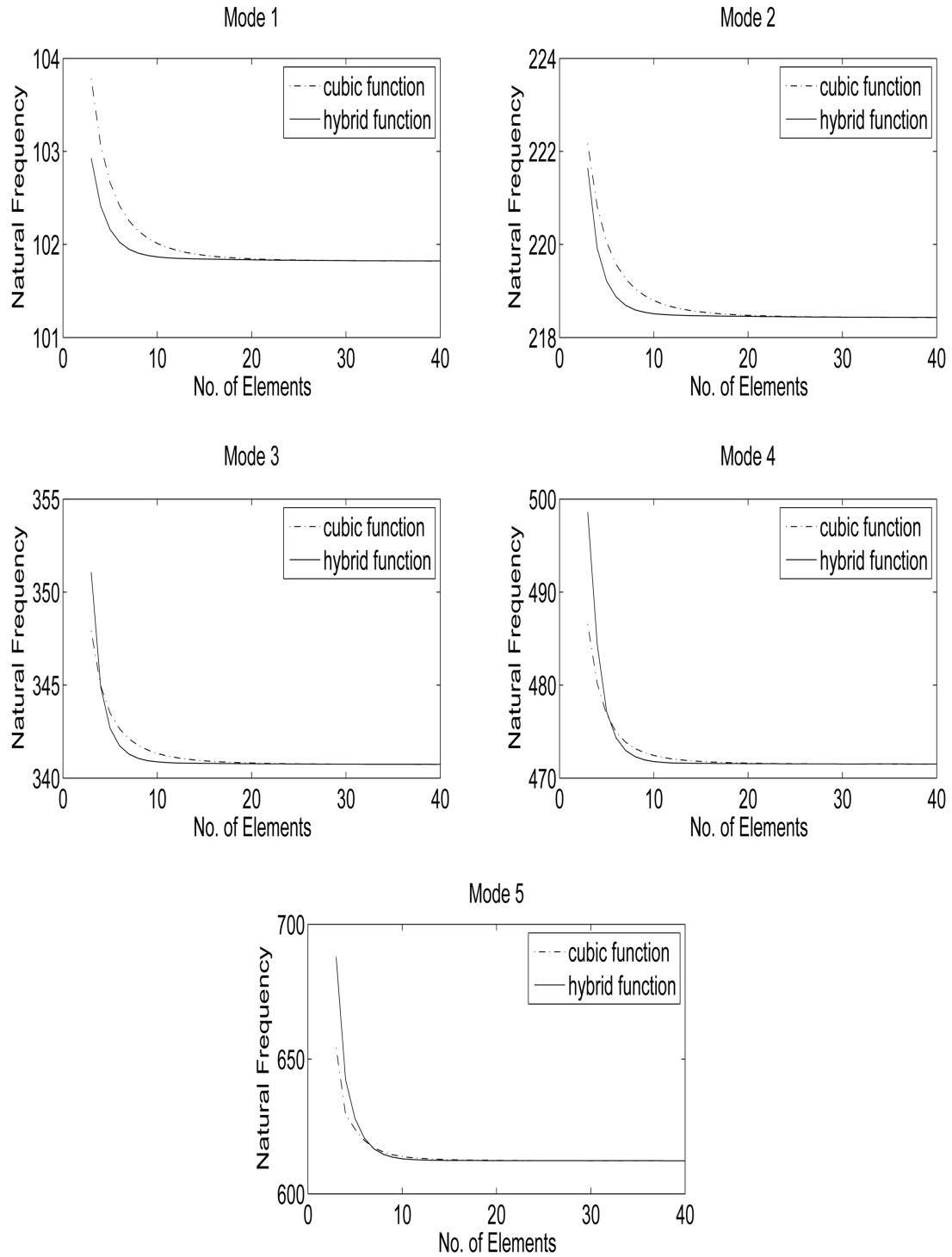
Fig. 10 Comparison of convergence of hybrid function and hermite cubic function for linearly tapered, linear flexural stiffness cantilever beam with $\lambda = 100$

Table 7 Comparison of non-dimensional frequencies for linear mass, cubic stiffness cantilevered rotating beam

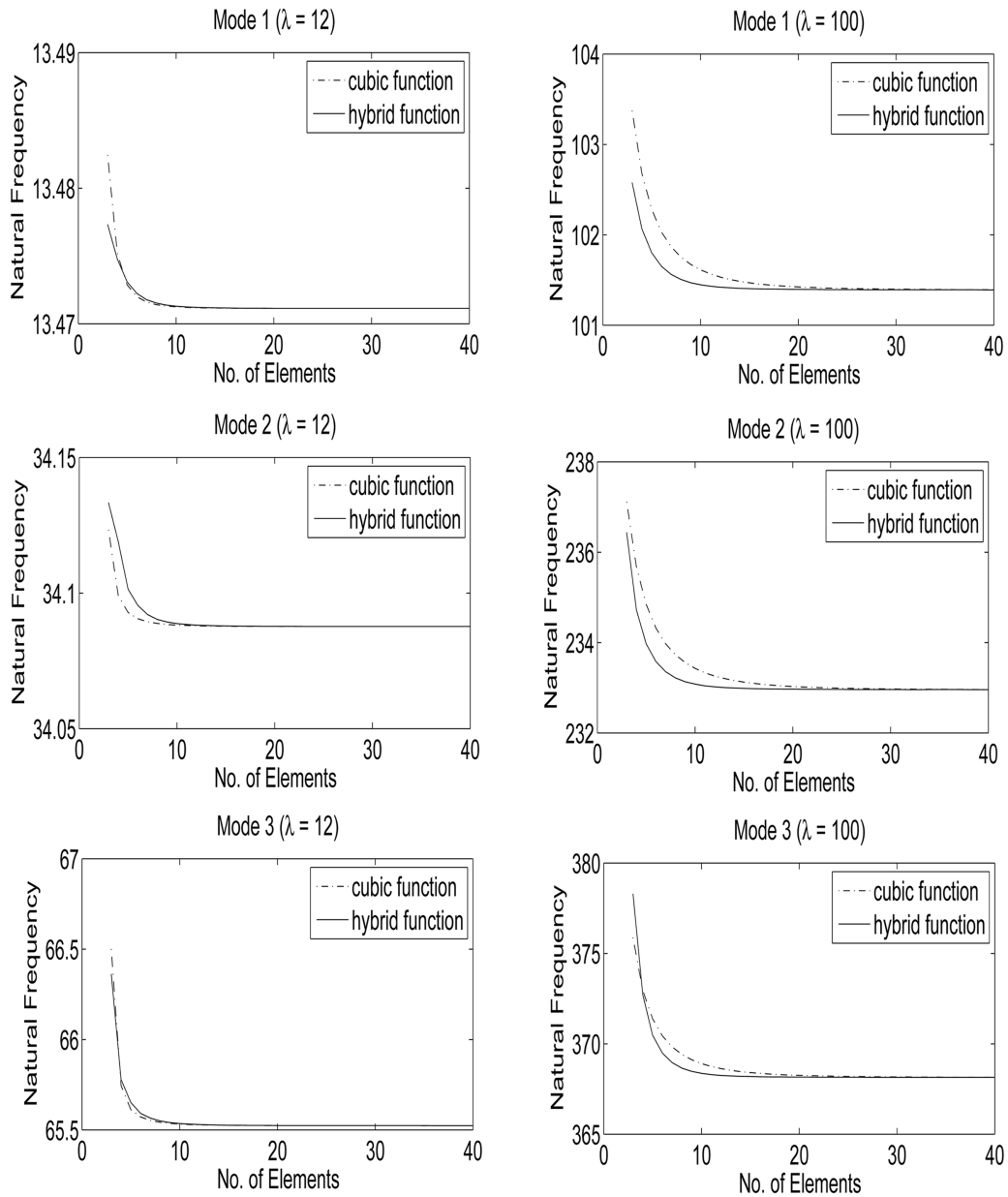| Mode	Present FEM	Wang and Wereley (2004)	Hodges and Rutkowsky (1981)
1	13.4711	13.4711	13.4711
2	34.0877	34.0877	34.0877
3	65.5237	65.5237	65.5237

Fig. 11 Comparison of convergence of hybrid function and hermite cubic function for linearly tapered, cubic flexural stiffness cantilever beam with $\lambda = 12$ and $\lambda = 100$

4.2.2 Linear mass and cubic stiffness beam

We assume $m(x) = m_0(1 - 0.5x)$ and $EI(x) = EI_0(1 - 0.95x)^3$. Table 7 shows comparison of non-dimensional rotating frequencies of a cantilever beam with results from (Wang and Wereley 2004, Wright *et al.* 1982). Values for the first three modes are only available in published literature. Again we see that the results compare very well.

Fig. 11 shows the comparison of the convergence rate of the current shape functions with the Hermite Cubic Shape functions. For the low speed case ($\lambda = 12$) the current basis function do not show an advantage compared to the cubic polynomial. However, in the higher speed case ($\lambda = 100$), the convergence is significantly improved.

4.3 Beams with hub offset

The new basis functions perform well for the test cases that have been used in published literature. Another advantage of the new basis function is that it is dependent of the hub offset. Even though the shape functions have been given for $R = 0$, hub offset can be included in the basis function. We expect the new basis function to perform better than the Hermite cubic function as hub offset increases the effect of the centrifugal force on the stiffness of the beam. Tables 8 and 9 show the natural frequencies for a cantilever rotating beam with linear mass and linear stiffness variation. Two different hub offset ratios R/L have been considered and the results have been validated with results from Wang and Wereley (2004); Wright *et al.* (1982). It is seen that the values for the first three modes compare very well.

Figs. 12-14 show the convergence trend observed by using the new basis function to determine the natural frequency of a high speed rotating beam with hub offset. The convergence trends are shown for the first three modes of the rotating beam for two hub offset ratios $R/L = 1\&5$. Furthermore, it is seen that, in the presence of hub offset, the new basis function shows a convergence trend which is almost independent of the geometric parameters of the rotating beam. This shows that there is a significant advantage in using the current basis function for high speed rotating beams.

Table 8 Comparison of non-dimensional frequencies for linear mass, linear stiffness cantilevered rotating beam for $\lambda = 5$ and $R/L = 1$

Mode	Present FEM	Wang and Wereley (2004)	Wright *et al.* (1982)
1	10.083	10.083	10.083
2	29.534	29.534	29.535
3	65.764	65.765	65.765

Table 9 Comparison of non-dimensional frequencies for linear mass, linear stiffness cantilevered rotating beam for $\lambda = 5$ and $R/L = 5$

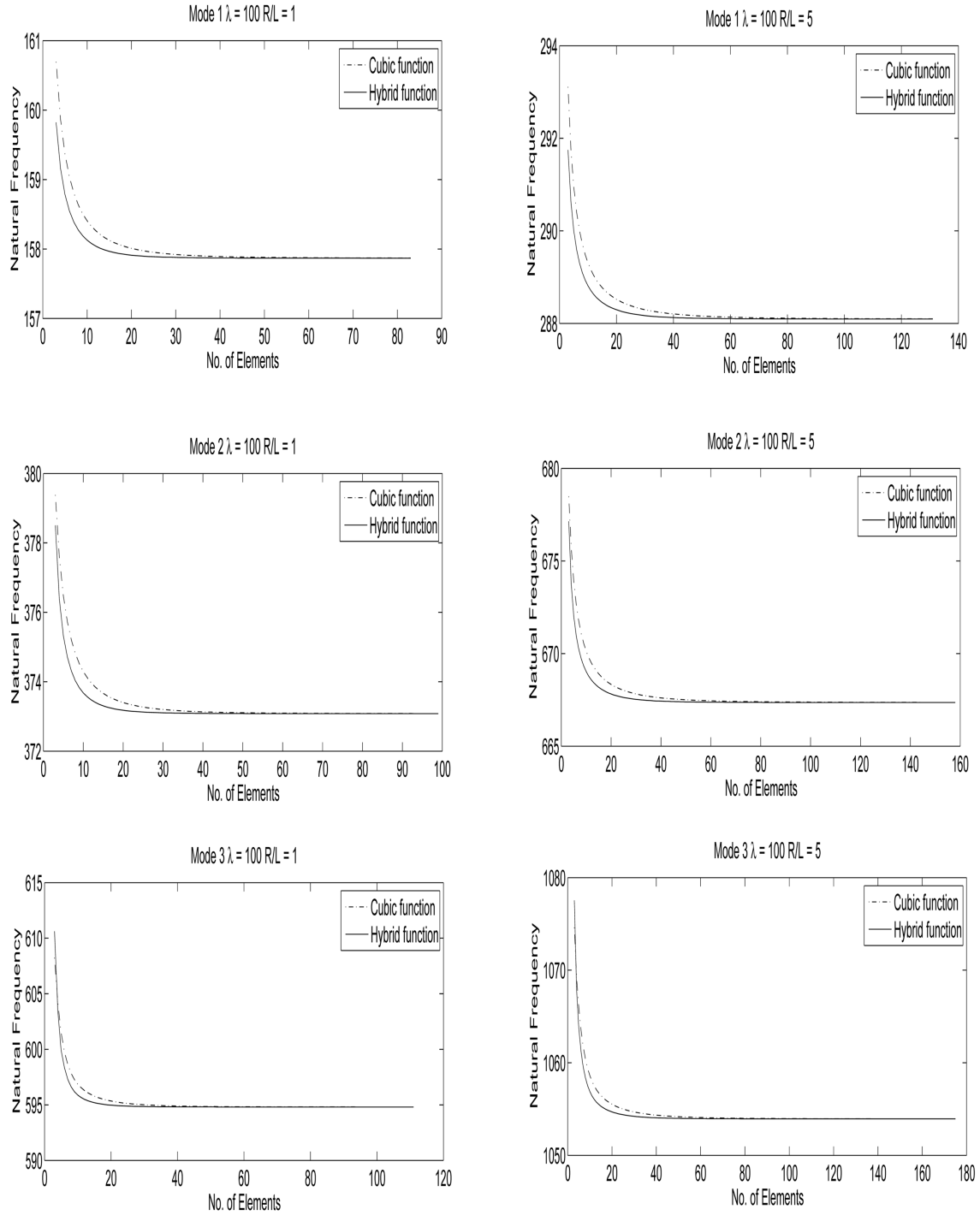| Mode	Present FEM	Wang and Wereley (2004)	Wright *et al.* (1982)
1	16.512	16.512	16.512
2	39.412	39.411	39.413
3	77.602	77.610	77.602

Fig. 12 Comparison of convergence of hybrid function and hermite cubic function for uniform cantilever beam with $\lambda = 100$ and $R/L = 1$ and 5
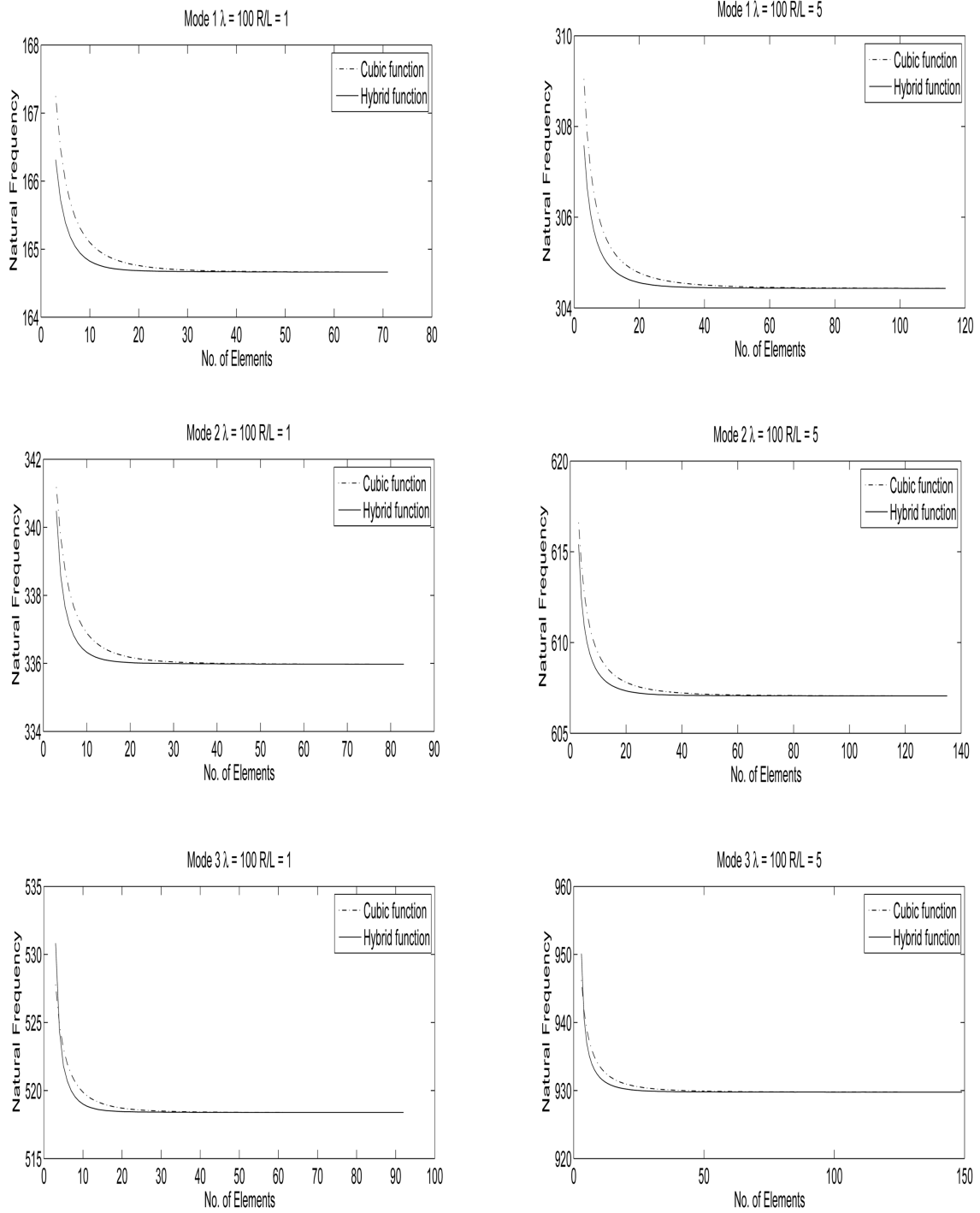
Fig. 13 Comparison of convergence of hybrid function and hermite cubic function for linearly tapered, linear flexural stiffness cantilever beam with $\lambda = 100$ and $R/L = 1$ and 5
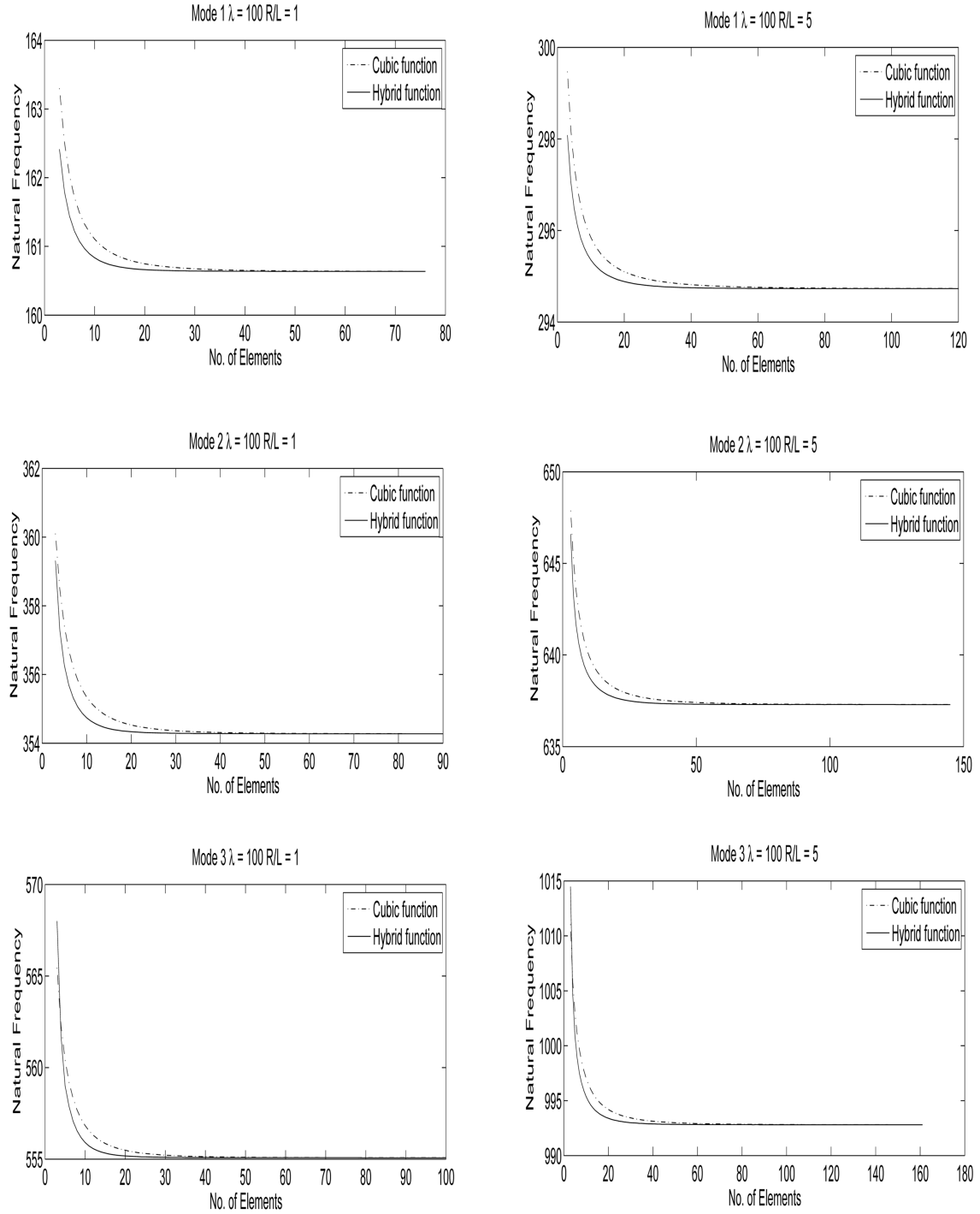
Fig. 14 Comparison of convergence of hybrid function and hermite cubic function for linearly tapered, cubic flexural stiffness cantilever beam with $\lambda = 100$ and $R/L = 1$ and 5

5. Conclusions

New basis functions are created to solve the free vibration problem for rotating beams and improve the accuracy and convergence of the finite element method. The problem physics of rotating beams requires that the centrifugal stiffening effects in the governing differential equation be properly captured by the basis functions. By assuming a linear combination of the solution to the two parts of the static part of the governing differential equation and forcing the error arising from the assumption to zero at collocation points within the domain, we generate new basis functions. The interpolation functions derived from this basis functions are a function of the element material and geometry parameters and of the speed of rotation. They also depend on the position of the element in the beam. They behave similar to the cubic interpolation functions for low rotation speeds and show better convergence rates as the rotation speed increases. The robustness of the functions is asserted by considering various cases of rotating beams and matching the obtained results with published literature. The new basis functions based on problem physics lead to a reduction in number of elements required for convergence by about 33% for high speed rotating beams. They are recommended for use for high speed rotating beams such as turbine blades and for control applications where reasonably accurate low order models are required.

References

Al-Qaisia, A. and Al-Bedoor, B. (2005), "Evaluation of different methods for the consideration of the effect of rotation on the stiffening of rotating beams", *J. Sound Vib.,* **280**(3-5), 531-553.

Banerjee, J.R. (2000), "Free vibration of centrifugally stiffened uniform and tapered beams using the dynamic stiffness method", *J. Sound Vib.,* **233**(5), 857-875.

Bathe, K.J. (1996), *Finite Element Procedures*, Prentice Hall.

Bauchau, O.A. and Hong, C.H. (1987), "Finite element approach to rotor blade modelling", *J. Am. Helicopter Soc.,* **32**(1), 60-67.

Bazoune, A. and Khulief, Y.A. (1992), "A finite beam element for vibration analysis of rotating tapered timoshenko beams", *J. Sound Vib.,* **156**(1), 141-164.

Bazoune, A., Khulief, Y.A. and Stephen, N.G. (1999), "Further results for modal characteristics of rotating tapered timoshenko beams", *J. Sound Vib.,* **219**(1), 157-174.

Chakraborty, A., Gopalakrishnan, S. and Reddy, J.N. (2003), "A new beam finite element for the analysis of functionally graded materials", *Int. J. Mech. Sci.*, **45**(3), 519-539.

Cook, R.D., Malkus, D.S., Plesha, M.E. and Witt, R.J. (2002), *Concepts and Applications of Finite Element Analysis*, John Wiley & Sons, New York.

Fallahi, B., Lai, S.H.Y. and Gupta, R. (1994), "Full beam formulation of a rotating beam-mass system", *ASME J. Vib. Acoust.,* **116**(1), 93-99.

Fox, C.H.J. and Burdess, J.S. (1979), "The natural frequencies of a rotating cantilever with offset root", *J. Sound Vib.,* **65**(2), 151-158.

Gunda, J.B. and Ganguli, R. (2008a), "New rational interpolation functions for finite element analysis of high speed rotating beams", *Int. J. Mech. Sci.*, **50**(3), 578-588.

Gunda, J.B. and Ganguli, R. (2008b), "Stiff-string basis functions for vibration analysis of high speed rotating beams", *J. Appl. Mech.,* **75**(2), 0245021-0245025.

Gunda, J.B., Singh, A.P., Chhabra, P.S. and Ganguli, R. (2007), "Free vibration analysis of rotating tapered blades using Fourier-p superelement", *Struct. Eng. Mech.*, **27**(2), 243-257.

Gupta, S. and Manohar, C.S. (2002), "Dynamic stiffness method for circular stochastic timoshenko beams: response variability and reliability analysis", *J. Sound Vib.*, **253**(5), 1915-1922.

Hamdan, M.N. and Al-Bedoor, B.O. (2001), "Non-linear free vibrations of a rotating flexible arm", *J. Sound*

Vib., **242**(5), 839-853.

Hashemi, S.M., Richard, M.J. and Dhatt, G. (1999), "A new dynamic finite element formulation for free lateral vibrations of Euler-bernoulli spinning beams using Trigonometric shape functions", *J. Sound Vib.,* **220**(4), 601-624.

Hildebrand, F.B. (1965), *Methods of Applied Mathematics*, Prentice Hall.

Hodges, D.H. and Rutkowski, M.J. (1981), "Free-vibration analysis of rotating beams by a variable- order finite element method", *AIAA J.,* **19**(11), 1459-1466.

Huang, K.J. and Liu, T.S. (2001), "Dynamic analysis of rotating beams with nonuniform cross sections using the dynamic stiffness method", *ASME J. Vib. Acoust.,* **123**(4), 536-539.

Kim, J. (2006), "Rotation effects on vibration of structures seen from a rotating beam simply supported off the rotation axis", *ASME J. Vib. Acoust.,* **128**(3), 328-337.

Lee, S.Y. and Kuo, Y.H. (1992), "Bending vibrations of a rotating non-uniform beam with an elastically restrained root", *J. Sound Vib.,* **154**(3), 441-451.

Lin, S.M. (2001), "The instability and vibration of rotating beams with arbitrary pretwist and an elastically restrained root", *ASME J. Appl. Mech.,* **68**(6), 844-853.

Lin, S.M. and Lee, S.Y. (2004), "Prediction of vibration and instability of rotating damped beams with an elastically restrained root", *Int. J. Mech. Sci.,* **46**(8), 1173-1194.

Naguleswaran, N. (1994), "Lateral vibration of a centrifugally tensioned uniform Euler-bernoulli beam", *J. Sound Vib.,* **176**(5), 613-624.

Pesheck, E., Pierre, C. and Shaw, S.W. (2002), "Modal reduction of a nonlinear rotating beam through nonlinear normal modes", *ASME J. Vib. Acoust.*, **124**(2), 229-236.

Pnueli, D. (1972), "Natural bending frequency comparable to rotational frequency in rotating cantilever beam", *J. Appl. Mech.,* **39**(2), 606-614.

Reddy, J.N. (1993), *An Introduction to the Finite Element Method,* 2nd Edition, McGraw-Hill, New York.

Subrahmanyam, K.B. and Kaza, K.R.V. (1987), "Non-linear flap-lag-extensional vibrations of rotating pretwisted, preconed beams including Coriolis effects", *Int. J. Mech. Sci.*, **29**(1), 29-43.

Udupa, K.M. and Varadan, T.K. (1990), "Hierarchical finite element method for rotating beams", *J. Sound Vib.,* **138**(3), 447-456.

Wang, G. and Wereley, N.M. (2004), "Free vibration analysis of rotating blades with uniform tapers", *AIAA J.,* **42**(12), 2429-2437.

Wright, A.D., Smith, C.E., Thresher, R.W. and Wang, J.L.C. (1982), "Vibration modes of centrifugally stiffened beams", *J. Appl. Mech.,* **49**(2), 197-202.

Wright, K. (2007), "Adaptive methods for piecewise polynomial collocation for ordinary differential equations", *BIT Numerical Mathematics* **47**, 197-212.

Yokoyama, T. (1988), "Free vibration characteristics of rotating Timoshenko beams", *Int. J. Mech. Sci.*, **30**(10), 743-755.

Notations

EI(*x*) : beam bending flexural stiffness
F   : axial force applied at the end of the beam
[**K**]   : global stiffness matrix
L   : length of the beam
l   : element length
[**M**]   : global mass matrix
m(*x*) : beam mass per unit length
n_e : number of elements
N   : shape functions
R   : offset length between beam and rotating hub
T   : kinetic energy
T(*x*) : beam axial force due to centrifugal stiffening
T_i(*x*) : beam axial force in each element due to centrifugal stiffening
U   : potential energy
w(*x*, *t*) : transverse displacement
x   : co-ordinate across the length of the beam
$\bar{x}$: co-ordinate across the length of the element
x_i : distance from root to left edge of ith element
λ   : non-dimensional rotation speed ($\lambda^2 = m\Omega^2 L^4/EI$)
Ω   : beam rotational speed
ω   : natural frequency
ξ   : non-dimensional beam length ($\xi = x/L$)